Development of an Automated Computer Vision Approach for Detonation Cellular Structure Analysis

Daniel Jalontzki, Shachar Charash, Alon Zussman
School of Mechanical Engineering, Tel Aviv University
Tel Aviv, Israel

Sumedh Pendurkar , Guni Sharon
Department of Computer Science & Engineering, Texas A&M University
College Station, Texas, USA

Yoram Kozak
School of Mechanical Engineering, Tel Aviv University
Tel Aviv, Israel

Supersonic detonation waves propagating through gaseous or heterogeneous mixtures of fuel and oxidizer can produce complex cellular structures. These detonation waves have numerous applications in engineering, such as rocket and jet propulsion with high thermal efficiency [1]. However, if not handled correctly, such detonations can be a safety hazard and lead to destructive explosions [2]. Consequently, a deep understanding of such detonation processes can both further their applicability and justify regulations for storage of liquid fuels in dedicated facilities [3]. Following these applications and safety concerns, and given the high-costs of real-world experiments, there is a need for reliable high-fidelity numerical simulations that can replicate real-world detonation conditions. One significant challenge that limits the validity of existing numerical simulation results is the uncertainty in their evaluation. Specifically, ambiguity in cell size measurements derived from both experimental and numerical soot foils. Common measurement methods, such as manual measurements, can display errors exceeding 50% [4]. Although different objective methods were suggested in the past, see [4–6], there is still no standard automated method for soot foil analysis.

Filling this gap, our work suggests a new method for cell size measurement and statistical analysis from soot foil images that is based on a computer vision approach. We present a fully automated cell size detection algorithm that consists of four primary steps: (1) image preprocessing, (2) cell contour detection, (3) parameter optimization, and (4) statistical analysis.

The first step applies image preprocessing techniques on a given soot foil image. Specifically, applying local contrast enhancement using *Contrast Limited Adaptive Histogram Equalization* (CLAHE), which make subtle features, such as cell boundaries and details within the cell structures, more distinguishable. Subsequently, a gray-scale dilation operation, which expands bright regions within the image, is performed on the contrast-enhanced image using a flat structuring element with dimensions of 8×8 pixels. Then, a pixel-wise division operation between the contrast-enhanced image and the dilated image is performed to normalize illumination variations in the image. Finally, the image undergoes thresholding

Correspondence to: danielj@mail.tau.ac.il

using *Otsu's method* [8]. This step converts the image into a binary format (0 for black and 1 for white), effectively distinguishing foreground and background based on intensity. Lastly, we perform non-local image denoising. Figure 1 demonstrates the image preprocessing, showing both an original soot foil image and the resulting manipulated image.

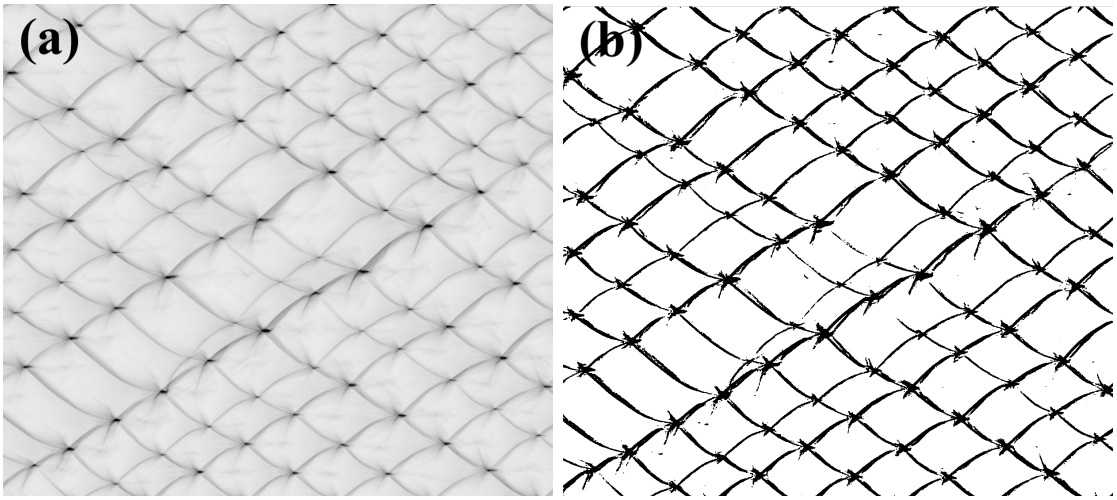

Figure 1: (a) Original numerical soot foil image, and (b) final output image after preprocessing stage.

Following preprocessing, the second step utilizes the *Suzuki and Abe* algorithm for cell contour detection [7]. However, this step may result in the identification of unwanted artifacts, as shown in Fig. 2a. To remedy this issue, the third step sets appropriate minimum and maximum area threshold values for the contour detection algorithm. As a result, structures that fall outside of this range are automatically filtered out. Thus, we aim to find these optimal minimum and maximum area values by using the proposed optimization algorithm. The algorithm utilizes a modified brute-force search over a range of minimum and maximum area values, $A_{\min}$ and $A_{\max}$, respectively. For this purpose, we define a junction as the situation where the bottom, left, top, and right corners of the top, right, bottom, and left cells, respectively, are found within a specified radius, $r = \sqrt{A/\pi}$, where A is the minimum or maximum area value. For each pair of values, following the contour detection procedure, the algorithm computes the total number of junctions. The optimal area values are those who yield the maximum number of junctions. Figure 2b shows the final resulting artifact-free soot foil image. Subsequently, the length and width of each identified cell are measured by determining the x and y coordinates of the right and left corners, and the top and bottom corners, respectively, and then calculating the Euclidean distance between each pair (in pixels). The final fourth step introduces statistical analysis, including a histogram of (1) cells size, (2) cells length, and (3) cells width, along with Cumulative Distribution Functions (CDFs) for each (normalized) histogram, and the average cell size (a scalar).

We demonstrate below the ability of the proposed computer-vision-based approach to automatically identify and measure detonation cell dimensions in [don't make a general claim. we can only make a specific claim. e.g., "in one representative numerical soot foil and one representative experimental soot foil] numerical and experimental soot foils. An example of a numerical soot foil image analysis is presented in Figs. 3-4. In particular, Fig. 3 illustrates the identification of cells in a nearly-regular patterned numerical soot foil (Fig. 3(a)) and the corresponding cell width and length measurements (Fig. 3(b)). These results show that the new approach can successfully detect cellular structures. Detailed statistical analysis based on these measurements is shown in Fig. 4. Specifically, Figs. 4a and 4b present histograms and Cumulative Distribution Functions (CDF), respectively, for both the cell width and length. Another example is shown in Figs. 5-6 for analysis of an irregular experimental soot foil

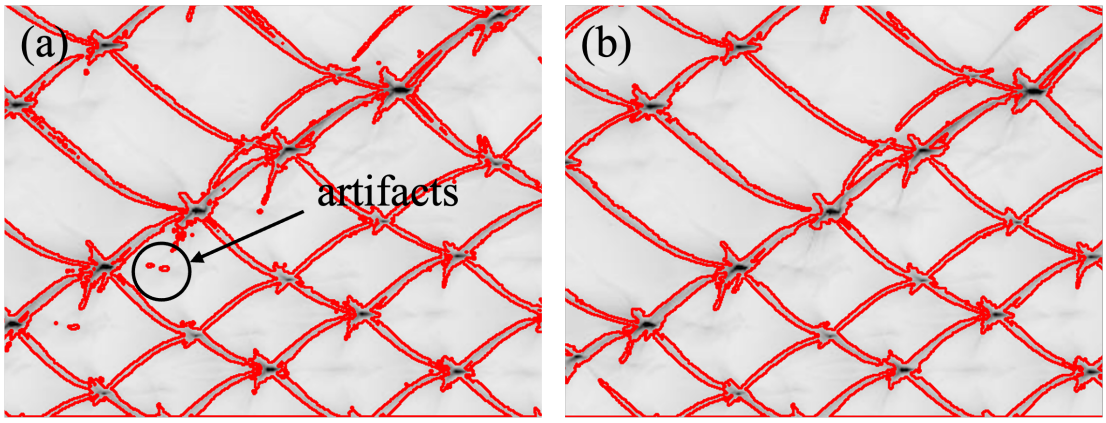

Figure 2: (a) Contour detection before applying area filtering, showing the identification of amorphous artifacts (an example is shown in circle), and (b) final contour detection image after optimization procedure.

from the work by Radulescu and Lee [9]. Figure 5a shows the contour detection algorithm results indicated in red color. Also, Fig. 5b presents the cell width and length measurements indicated by pink and green arrows, respectively. More detailed statistical analysis of both the cell width and length that includes histograms and CDFs is shown in Figs 6a and 6b, respectively. The aforementioned cases highlight the advantages of the proposed method for analyzing both numerical and experimental soot foil images with a wide range of cell regularity levels.

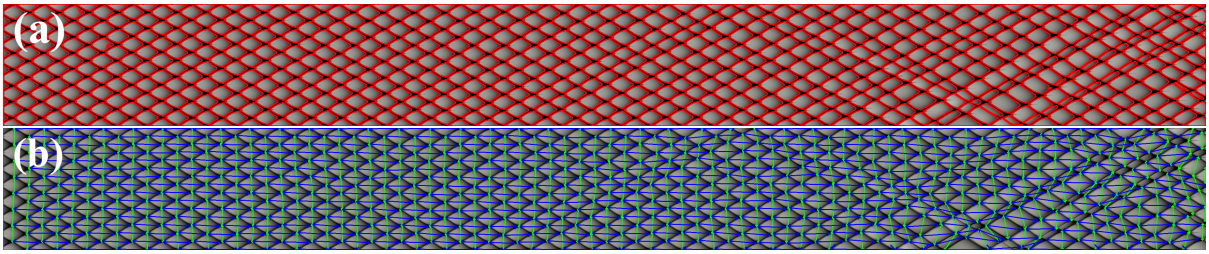

Figure 3: (a) Contour detection (red lines) of a nearly-regular numerical soot foil image, and (b) Computer vision approach cell width and length measurements.

We expect that the presented framework will contribute to standardization of detonation cell measurements and analysis. Future work will demonstrate and validate the applicability of the proposed approach across a variety of numerical and experimental soot foil images.

Acknowledgments

We would like to thank the U.S.-Israel Binational Science Foundation (BSF) for funding the research project “Modeling and Analysis of Heavy Hydrocarbon Liquid Fuel Spray Detonations”, Application Number: 2022191.

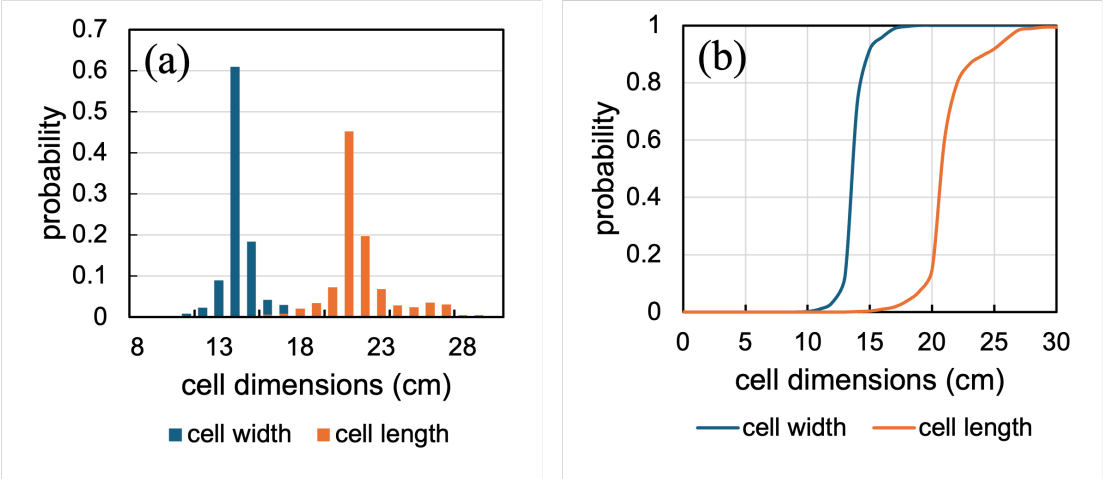

Figure 4: Statistical analysis for a nearly-regular numerical soot foil image, as shown in Fig. 3: (a) Histograms, and (b) CDF.

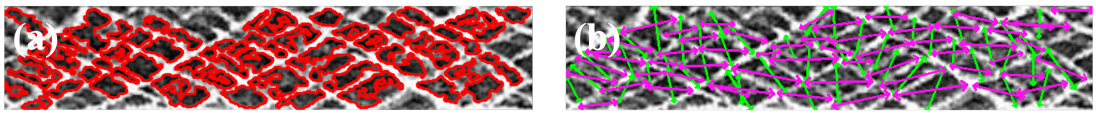

Figure 5: (a) Contour detection (red lines) of an irregular experimental soot foil image from [9], and (b) Computer vision approach cell width and length measurements (green and pink arrows).

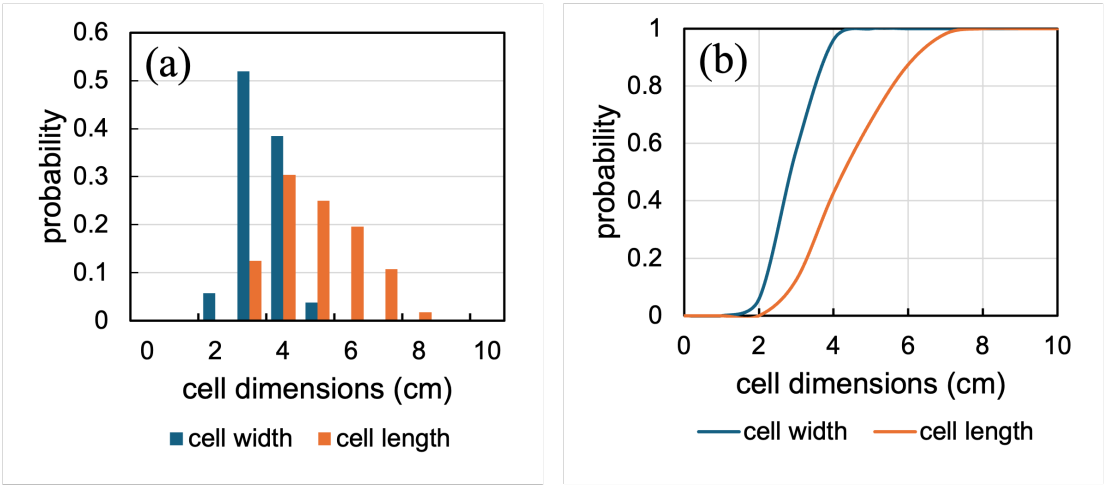

Figure 6: Statistical analysis for an irregular numerical soot foil image, as shown in Fig. 5: (a) Histograms, and (b) CDF.

References

[1] P. Wolański. (2013). Detonative propulsion, *Proceedings of the Combustion Institute*, vol. 34, no. 1, pp. 125-158. https://doi.org/10.1016/j.proci.2012.10.005

[2] S. Eidelman and A. Burcat. (1980). Evolution of a detonation wave in a cloud of fuel droplets. I - Influence of igniting explosion. *AIAA Journal*, 18(9), 1103-1109. https://doi.org/10.2514/3.7711

[3] E. S. Oran, G. Chamberlain, and A. Pekalski. (2020). Mechanisms and occurrence of detonations in vapor cloud explosions. *Progress in Energy and Combustion Science*, 77, 100804. https://doi.org/10.1016/j.pecs.2019.100804

[4] G. J. Sharpe and M. I. Radulescu. (2011). Statistical analysis of cellular detonation dynamics from numerical simulations: one-step chemistry. *Combustion Theory and Modelling*, 15(5), 691-723. https://doi.org/10.1080/13647830.2011.558594

[5] J. E. Shepherd, I. O. Moen, S. B. Murray, and P. A. Thibault. (1988). Analyses of the cellular structure of detonations. *Symposium (International) on Combustion*, 21(1), 1649-1658. https://doi.org/10.1016/S0082-0784(88)80398-9

[6] J. J. Lee, D. Garinis, D. L. Frost, J. H. S. Lee, and R. Knystautas. (1995). Two-dimensional autocorrelation function analysis of smoked foil patterns. *Shock Waves*, 5(3), 169-174. https://doi.org/10.1007/BF01435524

[7] S. Suzuki and K. Abe. (1985). Topological structural analysis of digitized binary images by border following. *Computer Vision, Graphics, and Image Processing*, 30(1), 32–46. https://doi.org/10.1016/0734-189X(85)90016-7

[8] N. Otsu. (1979). A threshold selection method from gray-level histograms, *IEEE Transactions on Systems, Man, and Cybernetics*, vol. 9, no. 1, pp. 62-66.

[9] M. I. Radulescu and J. H. S. Lee. (2002). The failure mechanism of gaseous detonations: experiments in porous wall tubes. *Combustion and Flame*, 131(1–2), 29–46. https://doi.org/10.1016/S0010-2180(02)00390-5